

RESEARCH

Open Access



Improving the quality of *Glycyrrhiza* stems and leaves through solid-state fermentation: flavonoid content, antioxidant activity, metabolic profile, and release mechanism

Juan Du^{1,2}, Xia Li^{1,3}, Na Liu^{1,2}, Yuan Wang^{1,2}, Yaqian Li^{1,2}, Yang Jia^{1,4}, Xiaoping An^{1,2*} and Jingwei Qi^{1,2*}

Abstract

Glycyrrhiza stems and leaves (GSL) are waste products of *Glycyrrhiza*; however, it has been considered a potential source of flavonoid compounds. In this study, GSL was processed by solid-state fermentation (SSF) to improve the flavonoid content and antioxidant activity. Firstly, a near-infrared (NIR) prediction model for flavonoid content in fermented *Glycyrrhiza* stems and leaves (FGSL) was established. Next, the effects of SSF on the antioxidant activity and metabolite profile of GSL were investigated. Finally, the possible mechanism of ferment release of flavonoids was explored based on enzyme activity, thermogravimetric analysis, and FTIR spectroscopy. The results revealed that NIR spectroscopy can efficiently analyze flavonoid contents in GSL, with predicted determination coefficient (R_p^2) and root mean square error (RMSEP) of 0.9874 and 0.125, respectively. SSF significantly increased the levels of flavonoids, and enhanced the scavenging activities of DPPH radical and hydroxyl radical and reducing power of FGSL. Widely targeted metabolomic analysis showed the detection of 461 differential metabolites were identified after SSF, with 141 metabolites remarkably up-regulated and 320 metabolites of FGSL down-regulated during fermentation. The main types of differential metabolites were phenolic acids and flavonoids, and the destruction of cellulose by SFF was crucial to the release of flavonoids. In conclusion, our study revealed that SSF remarkably improved the phytochemical components of FGSL by increasing enzyme activity and destroying cellulose structure, thereby contributing to the enhancement of antioxidant activity. This study provided a scientific basis for the production of high-value flavonoids from plant materials and offered a novel approach to elucidate the release and conversion of flavonoids.

Highlights

- We use a portable NIRS to screen the best FGSL.
- *Glycyrrhiza* stems and leaves flavonoids were improved after fermentation.
- The antioxidant activity of FGSL was increased after SSF.
- Metabolites difference between FGSL and GSL was investigated by metabolomic analysis.

*Correspondence:

Xiaoping An
xiaoping_an@163.com
Jingwei Qi
qjjingwei@imau.edu.cn

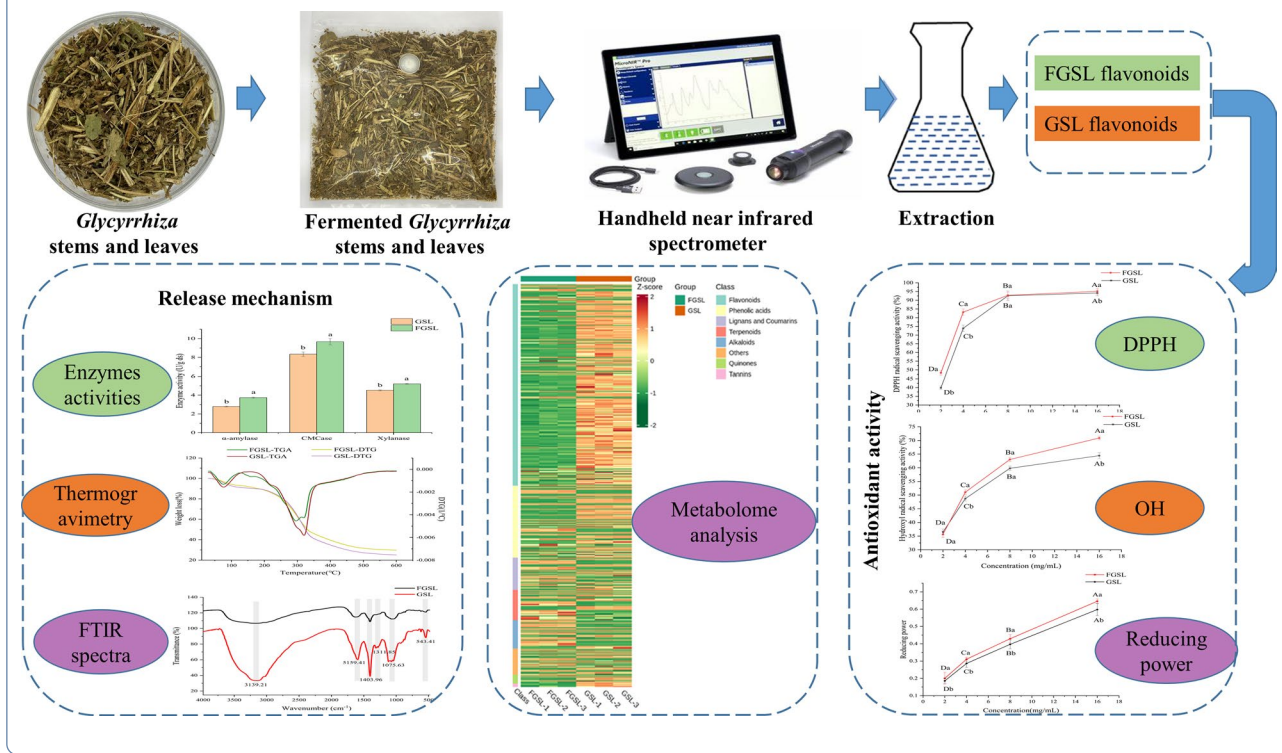
Full list of author information is available at the end of the article



© The Author(s) 2024. **Open Access** This article is licensed under a Creative Commons Attribution-NonCommercial-NoDerivatives 4.0 International License, which permits any non-commercial use, sharing, distribution and reproduction in any medium or format, as long as you give appropriate credit to the original author(s) and the source, provide a link to the Creative Commons licence, and indicate if you modified the licensed material. You do not have permission under this licence to share adapted material derived from this article or parts of it. The images or other third party material in this article are included in the article's Creative Commons licence, unless indicated otherwise in a credit line to the material. If material is not included in the article's Creative Commons licence and your intended use is not permitted by statutory regulation or exceeds the permitted use, you will need to obtain permission directly from the copyright holder. To view a copy of this licence, visit <http://creativecommons.org/licenses/by-nc-nd/4.0/>.

Keywords *Glycyrrhiza* stems and leaves, Flavonoids, Solid-state fermentation, Near-infrared spectroscopy, Antioxidant activities, Widely targeted metabolomics

Graphical Abstract



Introduction

Natural medicine, particularly natural herbal medicine, was well-known and concentrated on by our forefathers, and it was widely employed to cure various disorders. *Glycyrrhiza* (*Glycyrrhiza uralensis* Fisch.), a member of the *Leguminosae* family, is one of the most commonly used herbs globally, primarily in China’s Xinjiang and Inner Mongolia [1]. They are honored as “king of medicinal materials” in traditional Chinese medicine. In response to escalating market demands, *Glycyrrhiza* is now extensively cultivated across various regions in China, yielding an annual production exceeding 50,000 tons [2]. However, only the roots and rhizomes of *Glycyrrhiza* are used for medical purposes. The leaves and stems, which correspond to at least one-third of the total biomass of the plant, are usually considered agricultural wastes [3]. Moreover, numerous reports have also demonstrated that *Glycyrrhiza* stems and leaves contain abundant bioactive phytochemicals, such as triterpenoids, saponins, flavonoids, polysaccharides, coumarins, alkaloids, and proteins [2]. Among them, flavonoids are polyphenolic substances in large quantities in plants.

Their anti-oxidants, anti-inflammatory, anti-mutagenic, and anti-carcinogenic qualities made them essential ingredients for various nutraceutical, pharmaceutical, medical, and cosmetic uses [4]. However, earlier studies reported that the main bioactive components of plant materials, such as phenolic acids and flavonoids, are generally covalently esterified or conjugated bound to sugar residues and components of cell-wall, making them difficult to extract [5, 6]. Therefore, it is of great significance to explore the medicinal potential of *Glycyrrhiza* stems and leaves and improve its availability.

Solid state fermentation (SSF) is a technique that can enhance the value of medicinal plants as it releases flavonoids from the corresponding substrate and/or produces new flavonoids through secondary metabolism by microorganisms [7]. Numerous investigations have demonstrated that SSF significantly increased mulberry leaves’ flavonoid glycosides and biological activity [8, 9]. Ewers et al. [10] found that after SSF, the flavonoid concentration and antioxidant capacity of cinnamon’s flavonoid concentration and antioxidant capacity significantly increased. During this process, chemical analysis and

high-performance liquid chromatography (HPLC) are the conventional techniques used to measure the amount of flavonoids in fermentation sample materials. These techniques offer a high detection accuracy but also have limitations, including the inability to monitor on-site, costly technology, and a hefty workload [11]. However, the development of near-infrared spectroscopy (NIRS) is a quick, dependable, and reasonably priced solution that has drawn much interest from the food sector [12].

Therefore, the objective of this study was to detect and screen the best-fermented *Glycyrrhiza* stems and leaves in an economical, efficient, and nondestructive way by establishing a near-infrared spectroscopy prediction model for flavonoids content in fermented *Glycyrrhiza* stems and leaves (FGSL). Next, the in vitro antioxidant capacity and metabolites of *Glycyrrhiza* stems and leaves were compared with that of fermented *Glycyrrhiza* stems and leaves. Also, corresponding biotransformational pathways were elucidated by structural analyses, and evaluation of the activities of carbohydrate-hydrolyzing enzymes of the FGSL.

Materials and methods

Solid-state fermentation and sample preparation

The fermentation of *Glycyrrhiza* stems and leaves was carried out using a previous method [13]. Fresh *Glycyrrhiza* stems and leaves were collected in Hohhot, Inner Mongolia, China, in July after 3 years of cultivation of *Glycyrrhiza*. The aerial parts of *Glycyrrhiza* were air-dried, crushed to 3–5 cm, and used as the primary substrate for SSF. *Glycyrrhiza* stems and leaves were fermented in multi-layer polythene bags with a gas pressure opening valve. The fermentation medium contained 40 g of solid medium (*Glycyrrhiza* stems and leaves: maize meal: soybean meal: wheat bran=6:2:1:1) and 25 mL of distilled water and was inoculated with 0.2% of the compound probiotics (*Bacillus subtilis*, *Lactobacillus plantarum* and *Saccharomyces cerevisiae* mixed in the ratio of 1:1:1) and then fermented in a 30 °C incubator for 144 h. The fermentation specimens were sampled at 12 h intervals (0–144 h) with ten bags taken each time, and 130 samples were collected. It provided a representative set of *Glycyrrhiza* stems and leaves with different fermentation stages and was used to test the robustness of the NIR models as a function of the variability due to the sample quality and different fermentation levels. All the samples were dried at 45 °C and ground with a hammer mill. The best-fermented *Glycyrrhiza* stems and leaves predicted by the near-infrared technique were used for subsequent analysis.

A 1.0 g sample of GSL or FGSL was mixed with 50.0 mL of 50% ethanol and subjected to a temperature-controlled water bath at 80 °C for 60 min, followed by centrifugation

at a speed of 5000 rpm for 15 min [14]. The obtained supernatant was crude extracts of flavonoids from GSL and FGSL, and the content of flavonoids, antioxidant activity, and metabolomics were measured. Freeze dry the supernatant and perform infrared spectroscopy analysis.

NIR analysis

NIR spectroscopy measurement

This study used a handheld NIR spectrometer (Micro-NIR Onsite; Viavi; USA) to acquire spectral data. The wavelength range was 900–1700 nm, integration time was 0.1 ms, and scanning times were 100. As previously described, 13 sampling variables were established, each collecting ten sets of sample spectra. Each sample was subjected to three loading scans, and the average spectra of the three scans were considered the final analytical spectrum. Consequently, this resulted in 130 spectral data sets for further analysis.

Determination of total flavonoids

The flavonoid content was measured as reported previously [15]. Briefly, 2.5 mL of the samples were mixed with 0.4 mL of NaNO₂ (5%, w/v) for 6 min, followed by the addition and mixing of 0.4 mL of Al(NO₃)₃ (10%, w/v). After another 6 min, 2.0 mL of NaOH (1 M) was added to the solution, which was thoroughly mixed and incubated for 15 min. Finally, the absorbance at 510 nm was measured.

Reference data partition

It is essential to partition all samples into calibration and validation sets within an appropriate range to mitigate random errors and construct a more robust model. Initially, 130 *Glycyrrhiza* stems and leaves samples from various fermentation times were sorted in ascending order based on their chemical constituent values. Subsequently, out of every ten samples, the first, third, fifth, seventh, and ninth samples were allocated to the calibration set (a total of 65 samples). The prediction set, on the other hand, consisted of samples two, six, and ten (a total of 39 samples). Additionally, a complete external validation set comprising the fourth and eighth samples (26 in total) was employed to assess the effectiveness of the calibration model for prediction. (Table 1).

Spectral data processing

Sample surface inhomogeneities and ambient temperature can cause drift in spectral baselines, random noise, and spectral overlap during NIR. Preprocessing NIRS data can effectively remove the aforementioned phenomena, which is crucial for developing a robust and accurate model. Four different spectra processing techniques,

Table 1 Division of correction set and verification set of samples

Sample sets	Number	Maximum (N)	Minimum (N)
Gross sample	130	5.33	8.97
Calibration	65	5.30	8.94
Validation	39	5.31	8.97
External verification set	26	5.33	8.90

namely standard normal variate (SNV), Detrend correction (Detrend), first-order derivative (1st-der), and second-order derivative (2nd-der), were compared, respectively. Also, the combination of multiple methods for preprocessing was used in this study; these methods include 1st-der + SNV, 1st-der + Detrend, 2nd-der + SNV, 2nd-der + Detrend, SNV + Detrend, 1st-der + 2nd-der, 1st-der + SNV + Detrend, 2nd-der + SNV + Detrend, 1st-der + 2nd-der + SNV, 1st-der + 2nd-der + Detrend. In the end, 14 preprocessing methods were compared, and the coefficient of determination in calibration (R^2) was used to select the optimal preprocessing method.

Model evaluation

Typically, a superior model is assessed based on higher correlation coefficients for calibration (R_c^2), prediction (R_p^2), and residual predictive deviation (RPD), as well as lower root mean square errors for calibration (RMSEC) and prediction (RMSEP) [16].

Measurement of antioxidant activities

GSL and FGSL flavonoid extract solution (2, 4, 8, 16 mg/mL) was tested for DPPH radical scavenging activity, hydroxyl radical scavenging activity and reducing power. The antioxidant activity of the extract was assessed using the DPPH assay, as described by Wang et al. [17]. The ability of hydroxyl radicals scavenging was assessed using the method developed by Zhong et al. [18]. Additionally, the reducing power assay was conducted following a previously published method [19].

Widely-targeted metabolomics analysis

Based on previous studies [20], the UPLC-ESI-MS/MS system (UPLC, ExionLC™ AD, <https://sciex.com>) and a Tandem mass spectrometry system (<https://sciex.com.cn/>) were used to analyze the sample extract. The main operational parameters for the ESI source were as follows: the temperature of the source was set at 500°C; in positive ion mode, the ion spray voltage (I.S.) was adjusted to 5500 V, while in negative ion mode it was set to -4500 V; gas I (GSI), gas II (GSII), and curtain gas (CUR) pressures were maintained at 50, 60, and 25 psi respectively; collision-activated dissociation (CAD) was performed at a high level. QQQ scans were acquired as

MRM experiments with collision gas (nitrogen) set to medium D.P. (declustering potential) and C.E. (collision energy) for individual MRM transitions were done with further D.P. and C.E. optimization. A specific set of MRM transitions was monitored for each period according to the metabolites eluted within this period.

Determination of enzyme activity

The crude enzyme solution was obtained using the extraction method outlined by Chen et al. [21]. In brief, 2 g of FGSL or GSL powder was mixed with 20 mL of acetate buffer (pH 5.5, 0.1 M) and agitated at a speed of 200 rpm for one hour. Following this, the mixtures underwent centrifugation at a speed of 10,000×g for a duration of 10 min at a temperature of 4 °C in order to obtain the supernatants for subsequent. Carboxymethyl cellulase (CMCase), xylanase, and α-amylase levels were assessed using the DNS method at 540 nm.

FT-IR and thermogravimetric analysis

FTIR spectra were acquired with a FTIR spectrometer (Nicolet iS20, Thermo Fisher, USA). Samples were ground by mixing with KBr and then measured on the machine. The pyrolysis characteristics of cellulose were determined by TGA2 thermogravimetric analyzer (Mettler Toledo; Switzerland). The measured temperature was 25–600 °C, the heating rate was 10 °C/min, the gas was nitrogen, and the gas flow rate was 20 mL/min.

Statistical analysis

All the experiments were triplicated and the results were conveyed as means ± standard deviation. The data were subjected to analysis of variance (ANOVA) with the one-way ANOVA procedure in SAS (SAS; USA; ANOVA; significance level at $P \leq 0.05$). Relevant graphs were generated using Origin 2021 (Origin, Northampton, USA).

Results and discussion

Near infrared model construction and evaluation Flavonoid content changes during the fermentation of *Glycyrrhiza* stems and leaves

The flavonoid content was determined separately during the fermentation process of *Glycyrrhiza* stems and leaves based on chemometrics. The content was quantified by different degrees of fermentation, and the trend is shown in Fig. 1 while descriptive statistics are shown in Table 2, including range, mean and standard deviation (SD). The results indicate that the flavonoid content of fermentation *Glycyrrhiza* stems and leaves steadily increased until 3 d, reaching the maximum value at 72 h ($P < 0.05$). Compared with GSL, FGSL had significantly higher flavonoid contents ($P < 0.05$). This finding aligns with the findings of previous researchers who also observed that

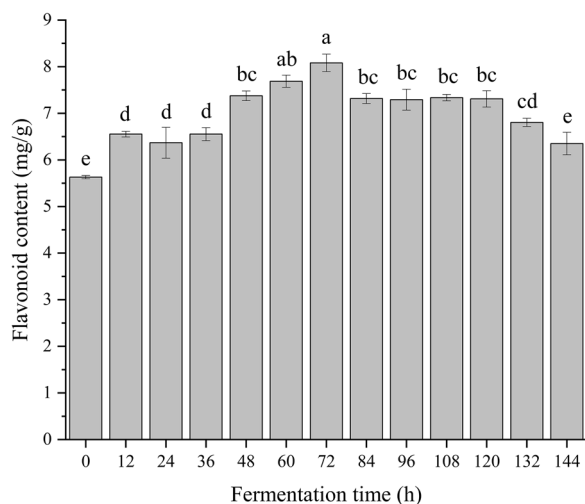


Fig. 1 Changes of flavonoid content in stems and leaves of *Glycyrrhiza* during fermentation. Different letters (a, b) above the columns indicated significant differences ($P < 0.05$)

Table 2 The descriptive statistical parameters of the flavonoid content in fermented *Glycyrrhiza* stems and leaves

Fermentation time (h)	Unit	Range	Mean	SD
0	mg/g	5.59–5.69	5.63	0.06
12	mg/g	5.33–5.86	6.55	0.21
24	mg/g	5.59–7.18	6.37	0.81
36	mg/g	6.02–7.39	6.55	0.48
48	mg/g	7.07–7.92	7.38	0.31
60	mg/g	7.18–8.55	7.69	0.45
72	mg/g	7.49–8.97	8.08	0.70
84	mg/g	6.86–7.71	7.32	0.32
96	mg/g	6–23–8.55	7.29	0.78
108	mg/g	7.18–7.49	7.34	0.14
120	mg/g	6.44–8.03	7.31	0.61
132	mg/g	6.23–7.28	6.80	0.34
144	mg/g	4.96–7.07	6.35	0.83

fermentation led to a rise in the overall flavonoid levels found in Chinese herbs [10, 22, 23]. The increase in flavonoid content of FGLS, as a result, may be due to microorganisms releasing a large amount of cellulases, pectinase, hemicellulose, and amylase during fermentation, which can effectively transform the insoluble-bound flavonoids into soluble forms and making it more bioavailable. In addition, from 84 h of fermentation, the flavonoid content of the FGLS continuously declined ($P < 0.05$) until the end of fermentation. This has also been observed by Wang et al. [22] in the fermentation of *Paeonia lactiflora* Root. This might be related to the rapid proliferation of

bacteria, which causes quicker consumption and modification of flavonoids, lowering overall flavonoid levels.

To establish a robust calibration set, it is essential to implement an appropriate experimental design. One of the fundamental principles is to ensure that the collected samples encompass property reference values across a relevant range, thereby capturing all anticipated sources of variance in the training data. Table 2 summarizes the detailed reference values of FGLS samples, significant differences were observed in the flavonoid content between stems and leaves of *Glycyrrhiza* at different fermentation times. The highest recorded flavonoid content was at 72 h, with an average value of 8.97 mg/g, while the lowest was observed at 144 h, with an average value of 4.96 mg/g. The fluctuation in flavonoid content in the stems and leaves of *Glycyrrhiza* indicates that the collected samples are representative and meet the requirement for a wide distribution of target contents in NIR quantitative models.

Spectral characteristics and preprocessing results

As shown in Fig. 2, typical spectra information of fermented *Glycyrrhiza* stems and leaves samples in the 1000–1800 nm wavelength range were collected using a portable NIR system. The raw spectra of 130 *Glycyrrhiza* stems and leaves samples showed similar tendencies, with notable absorption bands at 1200 nm, 1380 nm, and 1450 nm. These peaks represent overtone and combination bands related to C–H, O–H, and N–H. The absorption peak at 1200 nm indicates the presence of sugars and suggests the second overtone area of C–H bonds [24]. The absorption peaks at 1380 nm were connected to the first overtone of the C–H combination $-\text{CH}_2$ [25]. The absorption peak at 1450 nm is caused by the stretching vibration of the first-order frequency doubling of the water O–H group [26]. The identified absorption peaks within the 1000–1800 nm range are closely associated with the functional groups of flavonoids, enabling their utilization for analyzing catechins content and composition in fermented *Glycyrrhiza* stems and leaves. However, the original spectral data can be susceptible to various sources of noise interference, including high-frequency noise, baseline drift, and light scattering. To mitigate the impact of noise signals, several preprocessing techniques were employed on the original spectral curves. In this study, we employed four specific techniques, namely SNV, Detrend, 1st-der, and 2nd-der. Furthermore, a combination of these four methods was utilized to process the spectra as depicted in Fig. 3. The results showed that following preprocessing, the signal-to-noise ratio of the spectra had substantially improved and that appropriate spectra pretreatment was the critical guarantee for robust model creation and accurate prediction.

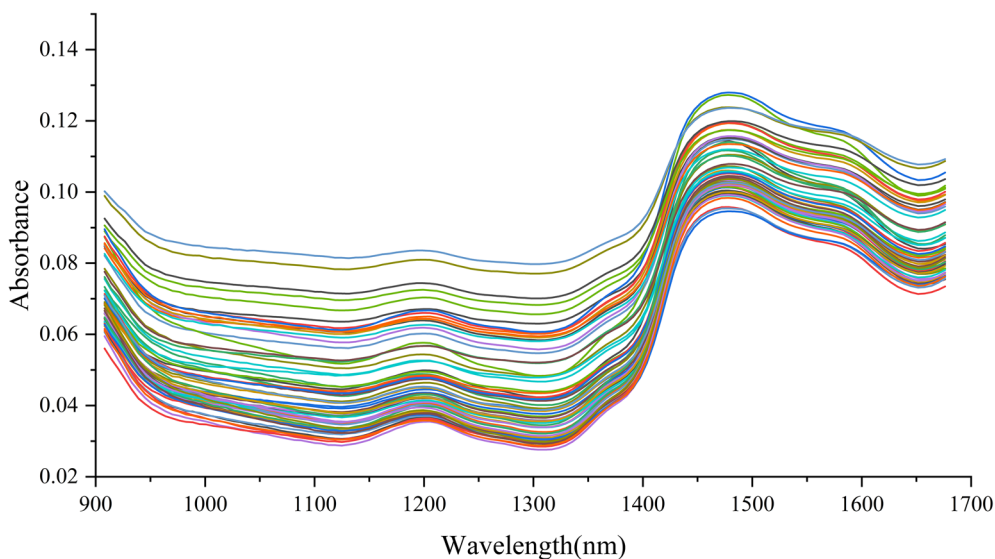


Fig. 2 Raw near-infrared spectra of fermented *Glycyrrhiza* stems and leaves

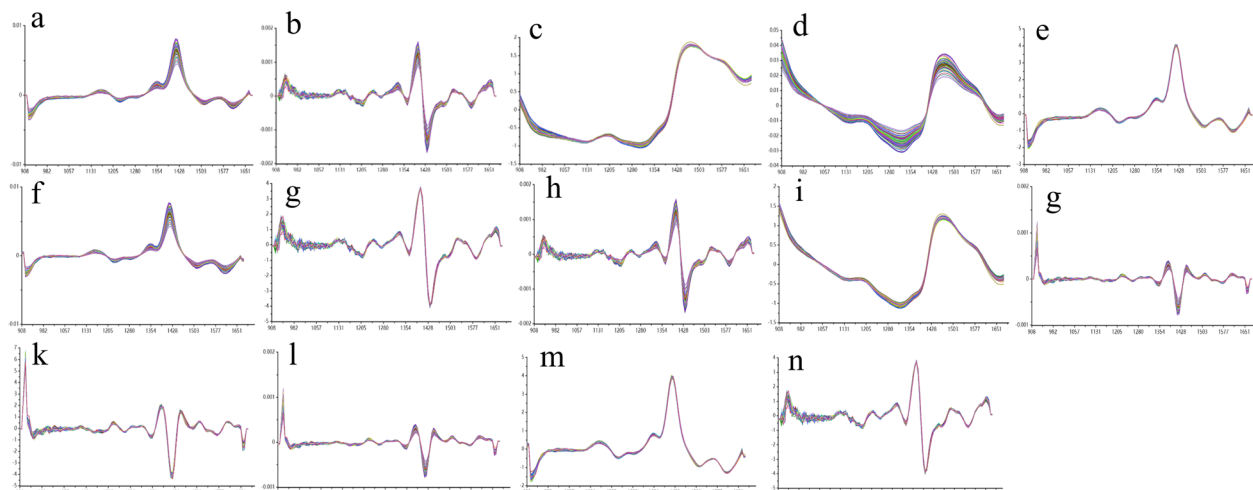


Fig. 3 Near-infrared pretreatment of fermented *Glycyrrhiza* stems and leaves. **a** 1st-der, **b** 2nd-der, **c** SNV, **d** Detrend, **e** 1st-der + SNV, **f** 1st-der + Detrend, **g** 2nd-der + SNV, **h** 2nd-der + Detrend, **i** SNV + Detrend, **j** 1st-der + 2nd-der, **k** 1st-der + 2nd-der + SNV, **l** 1st-der + 2nd-der + Detrend, **m** 1st-der + SNV + Detrend, **n** 2nd-der + SNV + Detrend

The PLSR model was built using the original spectrum and multiple preprocessing methods to determine the best spectral preprocessing strategy. Table 3 displays the comparable results. Based on the original spectral data, the correction set's correlation coefficient R_c^2 is 0.9757, RMSEC is 0.173, RPDc is 6.415, and the prediction set's correlation coefficient R_p^2 is 0.9763, RMSEP is 0.172, and RPDp is 6.496. Compared to the original spectrum, pretreatment significantly improved our model's performance. Out of all of them, the PLSR model that was created following the 2nd-der+SNV pretreatment has

the best prediction effect; R_c^2 is 0.9883, R_p^2 is 0.9874, and the RPD value is 8.909, indicating that the 2nd-der+SNV pretreatment can effectively reduce surface scattering and instrument noise-induced spectral error while also improving the model's accuracy. However, we also note that models that employ two spectral preprocessing techniques actually lead to reductions in the prediction model's accuracy. This implies that excessively intricate preprocessing designs could cause meaningful information from the spectral data to be lost in removing background interference, baseline drift, noise, and

Table 3 Effects of different spectral pretreatment methods on model performance

Pretreatment method	Calibration set			Prediction set		
	Rc ²	RMSEC	RPDc	Rp ²	RMSEP	RPDp
None	0.9757	0.173	6.415	0.9763	0.172	6.496
1st-der	0.9784	0.163	6.804	0.9735	0.165	6.14
2nd-der	0.9852	0.135	8.220	0.9873	0.133	8.874
SNV	0.9754	0.174	6.376	0.9775	0.172	6.667
Detrend	0.9838	0.141	7.857	0.9856	0.140	6.667
1st-der + SNV	0.9794	0.159	6.967	0.9729	0.160	6.075
1st-der + Detrend	0.9831	0.144	7.692	0.9832	0.143	7.715
2nd-der + SNV	0.9883	0.128	9.245	0.9874	0.125	8.909
2nd-der + Detrend	0.9872	0.125	8.839	0.9805	0.127	7.611
SNV + Detrend	0.9773	0.167	6.637	0.9734	0.169	6.131
1st-der + 2nd-der	0.9647	0.208	5.322	0.9623	0.209	5.150
1st-der + SNV + Detrend	0.9768	0.169	6.565	0.9752	0.170	6.350
2nd-der + SNV + Detrend	0.9848	0.136	8.111	0.9855	0.135	8.305
1st-der + 2nd-der + SNV	0.9672	0.201	5.522	0.9647	0.203	5.322
1st-der + 2nd-der + Detrend	0.9649	0.208	5.338	0.9611	0.212	5.070

color effects. Overall, pretreatment using 2nd-der + SNV resulted in the best model, which provided the greatest Rc² and Rp² and the least RMSEC and RMSECP, as well as RPDc and RPDp.

External validation

External validation: we further tested the model's resilience by using NIR technology on an independent prediction set of samples. Table 4 displays the predicted findings. The discrepancy between the predicted and measured values varies from -0.01 mg/g to 0.11 mg/g, and the prediction model's accuracy is excellent. As a result, the suggested method enables the direct determination of flavonoid concentration in Fermented *Glycyrrhiza* stems and leaves samples.

Antioxidant activity of GSL and FGSL

The amount of flavonoids in fermented *Glycyrrhiza* stems and leaves were much higher than in unfermented stems and leaves. Therefore, the high antioxidant effects of FGSL extracts in reducing power, hydroxyl radical scavenging activity, and DPPH radical scavenging activity (Fig. 4) are not surprising. The DPPH free extreme measurement is a reliable and stable qualitative solid free radical and a common in vitro antioxidant assessment technique. As can be shown in Fig. 4a, at dosages of 2, 4, 8, and 16 mg/mL, respectively, the DPPH free radical scavenging activity of FGSL rose to 48.31%, 83.21%, 92.87%, and 95.12%. Compared to GSL, FGSL showed much greater DPPH radical scavenging activity. One electron is lost from hydroxide in the molecular formula

Table 4 Comparison of measured and predicted flavonoid content in a complete external validation set

No	Flavonoid content (mg/g)		
	Experimental values	Predictive values	Error
S1	5.33	5.38	-0.05
S2	5.42	5.44	-0.02
S3	5.44	5.35	0.09
S4	5.45	6.47	-1.02
S5	5.55	5.57	-0.02
S6	5.64	5.69	-0.05
S7	5.76	5.85	-0.09
S8	6.37	6.35	0.02
S9	6.41	6.37	0.04
S10	6.78	6.74	0.04
S11	6.85	6.87	-0.02
S12	7.15	7.14	0.01
S13	7.17	7.06	0.11
S14	7.78	7.79	-0.01
S15	7.76	7.78	-0.02
S16	7.68	7.66	0.02
S17	7.67	7.73	-0.06
S18	7.51	7.56	-0.05
S19	7.65	7.66	-0.01
S20	8.02	8.07	-0.05
S21	8.09	8.16	-0.07
S22	8.54	8.55	-0.01
S23	8.63	8.66	-0.03
S24	8.84	8.75	0.09
S25	8.90	8.88	0.02
S26	8.88	8.84	0.04

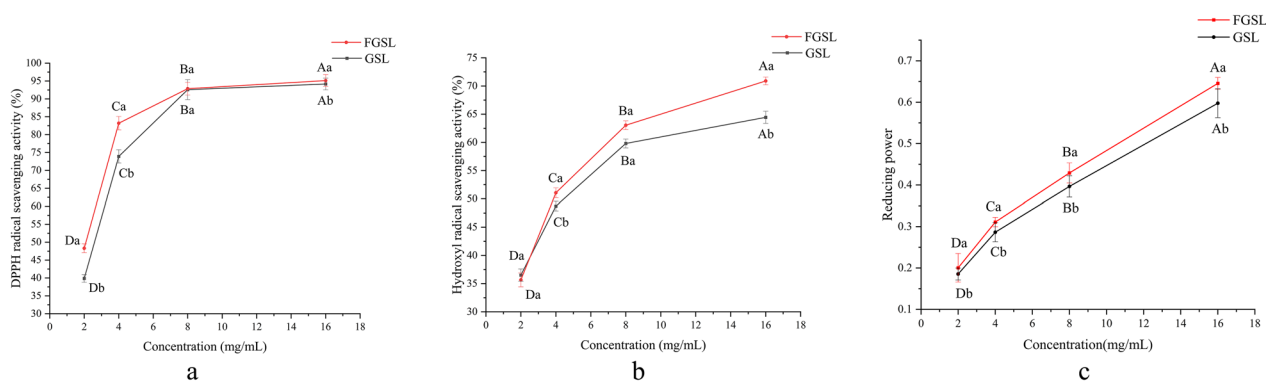


Fig. 4 DPPH radical scavenging activity (a), hydroxyl radical scavenging activity (b) and reducing power (c) of FGSL and GSL. Different uppercase letters indicate significant differences between groups with different concentrations ($P < 0.05$). Lowercase letters indicate significant differences between groups with different samples ($P < 0.05$)

to produce the hydroxyl radical, a prominent reactive oxygen species. Due to their potent oxidizing capability, hydroxyl radicals can readily traverse cellular membranes and interact with biological molecules, thereby contributing to cellular demise and tissue harm. Thus, scavenging hydroxyl radicals protects living systems [27]. As illustrated in Fig. 4b, FGSL and GSL exhibited apparent scavenging effects on the hydroxyl radicals in a dose-dependent manner at concentrations from 2 to 16 mg/mL. Furthermore, FGSL exhibited significantly more vigorous hydroxyl radical scavenging activity than GSL. When the concentration approached 16.0 mg/mL, the hydroxyl radicals scavenging rate of FGSL was 70.90%, significantly higher than that of GSL (55.65%). The increased free radical scavenging rate of the FGSL might be attributed to the significant production of total flavonoids and total phenols, and microbial metabolism can enhance the compounds with proton-donor properties, leading to an increased ability to scavenge free radicals [28]. These results are consistent with the study conducted by Liu et al. [20], which reported that dandelion exhibits higher DPPH and hydroxyl radical scavenging abilities after SSF. The reduction capability level of compounds represented the electron donor capability of antioxidant substances. The stronger the reduction capability, the stronger the antioxidant capability of samples [29]. As seen in Fig. 4c, there was a correlation between the reducing power of FGSL and GSL and the concentration, with FGSL having a higher reducing power than GSL ($P < 0.05$). When the concentration was 16 mg/mL, the reducing power of FGSL and GSL was 0.65 ± 0.01 and 0.59 ± 0.03 , respectively. The reduction ability of FGSL was significantly improved, which showed that there were more antioxidants in the FGSL that could scavenge radicals. This indicated that the reduction ability of GSL can be improved by fermentation treatment. This result

was similar to previous research results. Li et al. [29] reported that the fermentation of oat bran with *Lactobacillus fermentum* NBO2 increased the release of phenolic compounds, and the reducing power of the fermentation group was higher than that of the unfermented. Furthermore, Guo et al. [8] indicated that the antioxidant capabilities of fermented mulberry leaves were largely linked to their flavonoid content, with the scavenging augmented with a rise in flavonoid contents, demonstrating previous findings. In conclusion, fermentation treatment can effectively increase the release of flavonoids and polyphenols in GSL, thereby improving its antioxidant activity.

Widely targeted metabolomics analysis

Multivariate analysis

To comprehensively analyze the metabolite variations before and after fermentation, we employed a UPLC-MS/MS system to perform widely targeted metabolomics on FGSL and GSL. The results of quality control samples were visually presented through overlapping display analysis of the total ion current (TIC) in Fig. 5a, b. The consistent retention time and peak intensity within each group indicated our instrument's stability and our data's reliability. Furthermore, PCA was employed to investigate the differences in metabolites between the two groups and the degree of variation within each group. The results are presented in Fig. 6a, b as two-dimensional and three-dimensional scatter plots. PC1 accounted for 65.11% of the total variance, while PC2 explained 11.38%. This analysis effectively distinguished fermented from unfermented samples, indicating that fermentation alters flavonoid profiles in *Glycyrrhiza* stems and leaves. Moreover, there was minimal variation among replicates, demonstrating good sample repeatability.

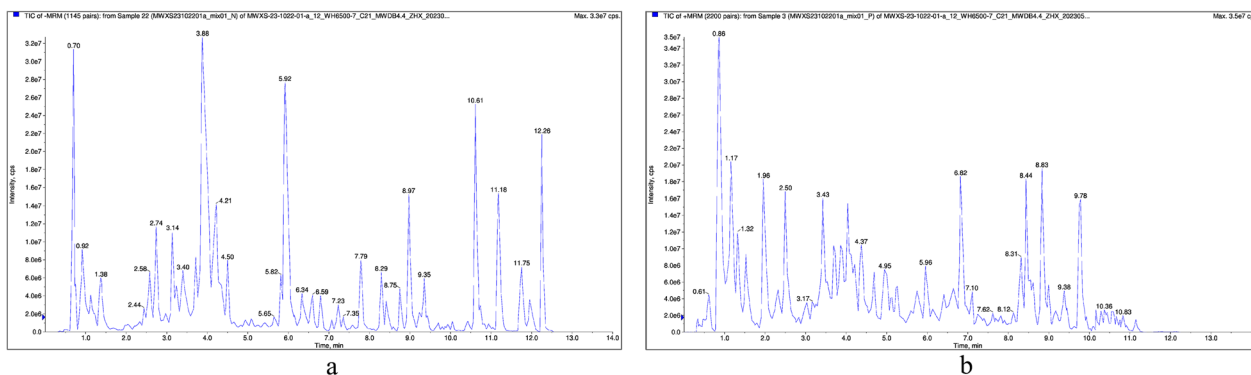


Fig. 5 Total ions current (TIC) overlapping map of Q.C. samples mass spectrometry results. The abscissa is the retention time of the metabolite detection. The ordinate is the ion current intensity of the ion detection (the intensity units are counts per second (cps)). **a** In negative ion mode, **b** in positive ion mode

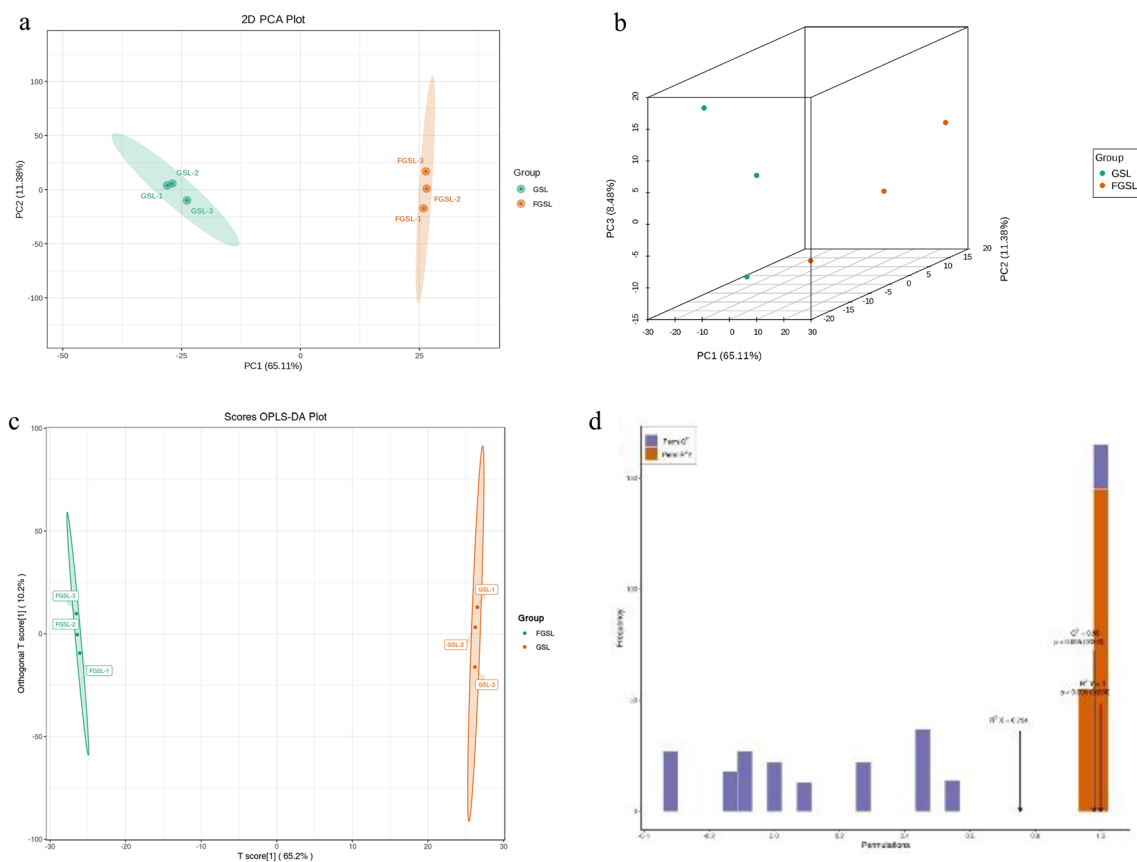


Fig. 6 Multivariate analysis of metabolomics data on fermented and unfermented Glycyrrhiza stems and leaves. **a** The two-dimensional scatter plot of the PCA model of two groups. **b** The three-dimensional scatter plot of the PCA model of two groups. **c** The scatter plot of the OPLS-DA model. **d** OPLS-DA validation diagram

The OPLS-DA model, a supervised pattern recognition approach using multivariate statistical analysis, was employed to distinguish groups effectively and identify differential metabolites. The OPLS-DA model score plot

(Fig. 6c) demonstrated distinct separations between the FGSL and GSL groups, indicating significant differences in metabolite profiles. Q^2 represents the model's prediction ability, while R^2Y and R^2X reflect the interpretation

rate for Y and X matrices, respectively. As shown in Fig. 6d, the values of R^2X (cum), R^2Y (cum), and Q^2 were determined as 0.895, 1.000, and 0.998, respectively, suggesting that this model is appropriate [30, 31]. Additionally, to further validate our findings' reliability, we conducted 200 random permutation tests on the OPLS-DA mode, which yielded a P -value lower than 0.005. These results collectively support the robustness of our chosen OPLS-DA model for investigating metabolic changes between FGSL and GSL.

Screening of differential metabolites

To quickly assess the differences in metabolite expression levels between the two groups and determine their statistical significance, we utilized variable projection (VIP) > 1.0, $P < 0.05$, and $|\text{Log}_2\text{FC}| > \text{onefold change (F.C.)}$ as criteria. The volcano plot shows the differential metabolites (Fig. 7a). Compared with GSL, 141 metabolites of FGSL were substantially upregulated, and 320 metabolites were substantially down-regulated. These metabolites included, in detail, 251 flavonoids, 90 phenolic acids, 38 terpenoids, 40 lignans and coumarins, 35 alkaloids, and 33 additional metabolites. The heat map (Fig. S1) shows the dynamic fluctuations of these metabolites. Phenolics and flavonoids were the primary differential metabolites. (Fig. 7b and Table S1). SSF can effectively enhance Glycyrrhiza stems and leaves flavonoids, such as Glabrol, Isobavachalcone D, (2S)-Abyssinone II, Luteolin-6,8-di-C-arabinoside, Kaempferol-7-O-rhamnoside,

3',4',6-Trihydroxyaurone, Kaempferol-3-O-rhamnoside (Afzelin) (Kaempferin) and Chrysin, as well as the relative content of Ethyl ferulate and 3,4-Dimethoxycinnamic acid in FGSL significantly increased compared to that in GSL. Additionally, several soluble bioactive chemicals may be created during SSF and are secondary metabolites of microbes, including phenolics, flavonoids, and organic acids [32].

KEGG annotation and enrichment analysis of differential metabolites

We conducted pathway enrichment analysis using the KEGG database to understand better the pathways associated with the metabolites that showed differential expression. The results of this analysis were visualized in bubble plots (Fig. 8). Our findings revealed that the metabolites affected by fermentation were involved in 26 specific pathways. Notably, our top three highest-impact pathways included folate biosynthesis, flavone and flavonol biosynthesis, and isoflavonoid biosynthesis. These pathways are essential for synthesizing flavonoids, phenolic, and amino acids. This suggests that fermentation enhanced existing flavonoid content in Glycyrrhiza stems and leaves and stimulated the production of new flavonoid compounds. Further investigation is required to understand how fermentation influences the abundance of these flavonoid metabolites. Additionally, we observed close structural and biochemical relationships

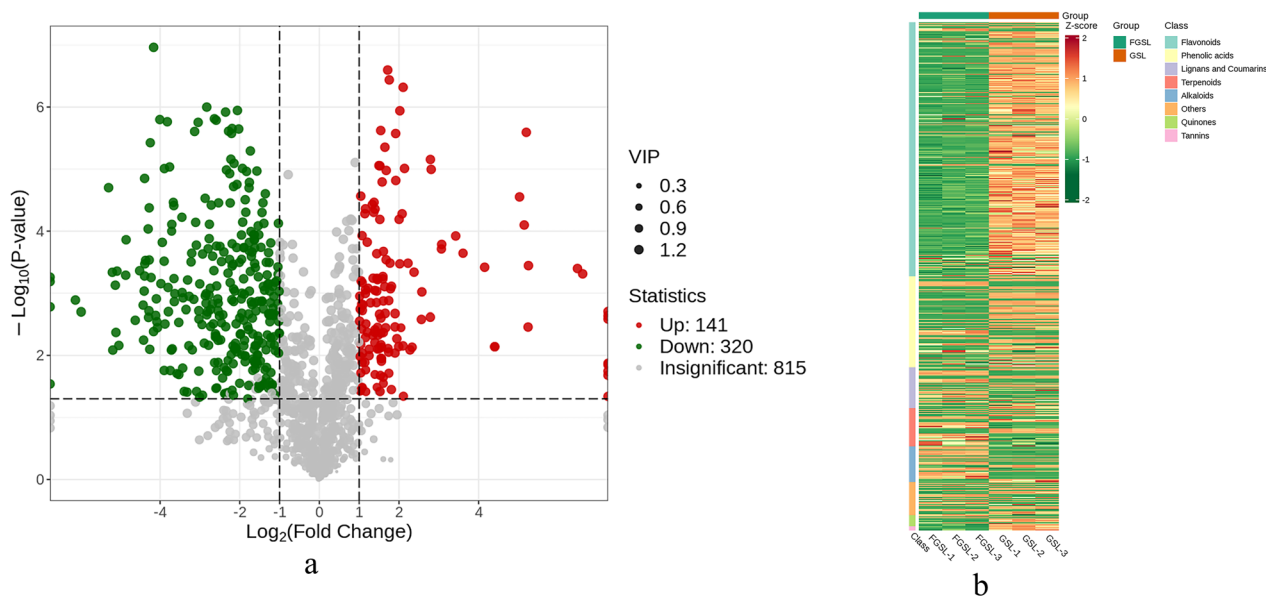


Fig. 7 Chemical differences between fermented and unfermented Glycyrrhiza stems and leaves. **a** The volcano plot shows the differential metabolite expression levels in FGSL and GSL samples. Red, green, and grey dots indicate upregulated, downregulated, and insignificant differentially expressed metabolites. **b** Differentially expressed metabolites' heatmap of hierarchical clustering analysis for FGSL and GSL

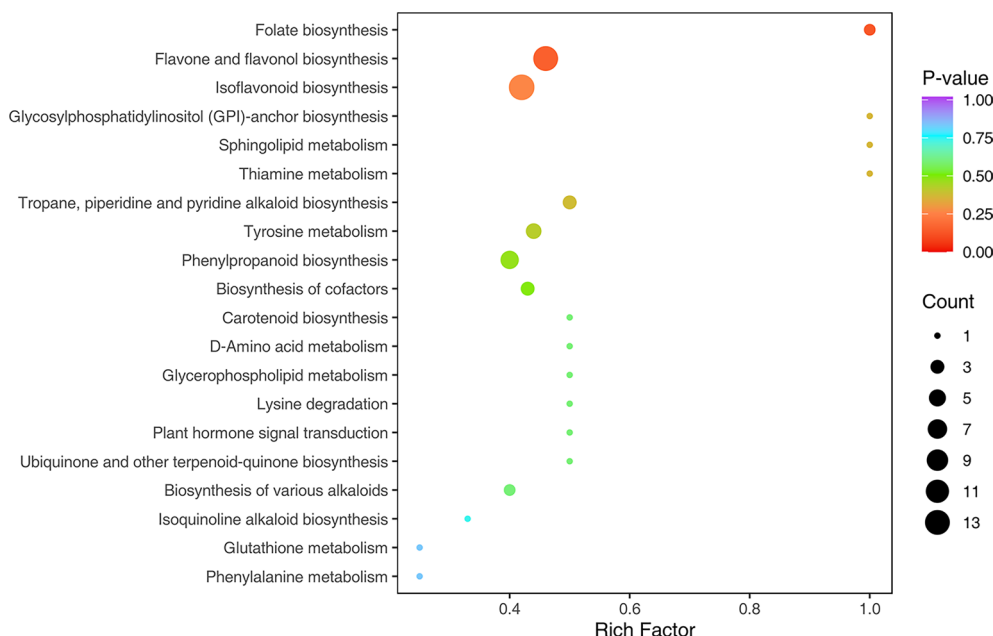


Fig. 8 KEGG pathway enrichment of the differentially accumulated metabolites between fermented and unfermented *Glycyrrhiza* stems and leaves. Each bubble in the plot represents a metabolic pathway whose abscissa and bubble size jointly indicate the magnitude of the impact factors of the pathway. The bubble colours represent the p-values of the enrichment analysis, with darker colours showing a higher degree of enrichment

among these differential metabolites, which may explain their increased levels during fermentation.

Release mechanism of flavonoids

Enzymes activities

Lignin is interwoven with cellulose and hemicellulose to create lignin carbohydrate polymers, and compound degradation is primarily dependent on carbohydrate hydrolases generated by microbial fermentation [33]. The activities of CMCase, xylanase, and α -amylase were examined in this study. CMCase, xylanase, and α -amylase

activities were significantly elevated during SSE, as indicated in Fig. 9a. The cellulase enzyme, acting as a cell wall degrader, serves a dual purpose: firstly, it breaks down cellulose or oligosaccharides into glucose to participate in fermentation; secondly, its degradation disrupts the overall structure of the cell wall and facilitates the release of insoluble-bound phenolic fractions. By randomly breaking internal α -1,4-glucosidic connections, the α -amylase enzyme may hydrolyze starch, glycogen, and other related polysaccharides to produce oligosaccharides of different sizes [34]. This enzymatic process may result in

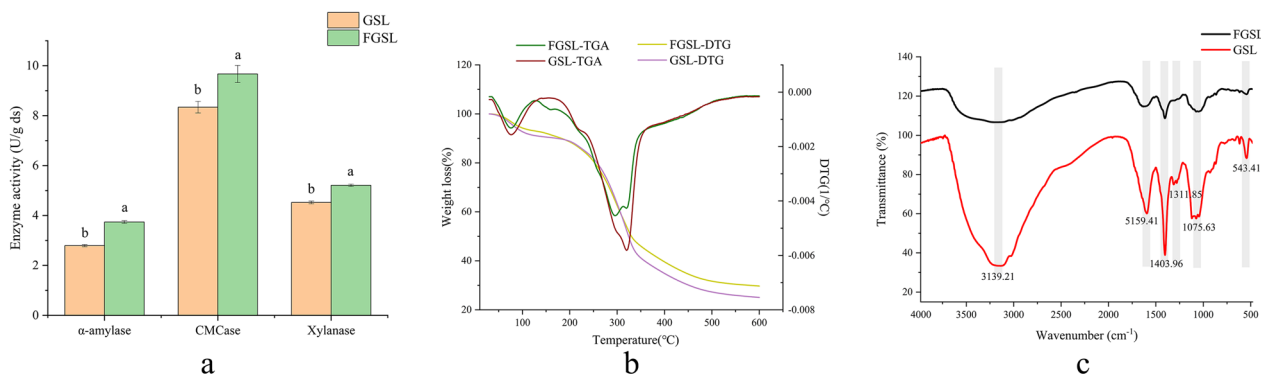


Fig. 9 Investigation of the release mechanisms of flavonoids. **a** Enzymatic activities; **b** thermogravimetric analysis (TGA thermogravimetric analysis, DTG derivative thermogravimetry curve); **c** FT-IR analysis

the release of phenolic compounds conjugated with the polysaccharides.

Additionally, the produced oligosaccharides are an energy source to support microbial enzymatic liberation of phenolic fractions [35, 36]. Xie et al. [37] discovered that xylanase production from *Trichoderma viride* during SSF was required to release bound polyphenols of insoluble dietary fiber. Xiao et al. [38] used probiotic fermented buckwheat and produced β -glucosidase, α -amylase, and CMCase, significantly improving the phytochemical composition of buckwheat and enhancing its antioxidant activity. According to the data above, it is indicated that CMCase, xylanase, and α -amylase play essential roles in the release and transformation of phenolics in *Glycyrrhiza* stems and leaves during fermentation, leading to the enhancement of flavonoid components and antioxidant activity in fermented *Glycyrrhiza* stems and leaves.

Effects of SSF on the thermal properties of *Glycyrrhiza* stems and leaves

Combined with TGA and derivative thermogravimetry (DTG) curves (Fig. 9b), the mass loss of the two samples can be divided into three main stages. The temperature range of the first stage was 30–220 °C, mainly due to the evaporation of free and crystal water in the sample [39]. The temperature range of the second stage was 220–400 °C, and decomposition peaks were observed at temperatures ranging from 246 to 260 °C and from 300 to 345 °C. These peaks corresponded to the breakdown of hemicellulose and cellulose, respectively. The absence of a cellulose decomposition peak in the DTG curves of FGSL could be attributed to potential structural changes in cell walls caused by SSF, leading to a significant reduction in the cellulose content present in FGSL. The substantial reduction of cellulose resulted in dissociation of some binding bioactive components, including representative components such as phenolic acids and flavonoids [9]. The third stage undergoes a biological carbonization process, with a degradation temperature ranging from 500 to 600 °C. The weight loss of FGSL was greater than that of GSL during the thermal degradation process, particularly within the temperature range of 300 to 600 °C. The thermal stability of the FGSL sample was observed to decrease, primarily due to the disruption in its crystal structure caused by SSF [40].

Effects of SSF on the functional groups and chemical bonds of *Glycyrrhiza* stems and leaves

The FTIR spectra were used to examine the differences in functional groups and chemical bonds between fermented and unfermented *Glycyrrhiza* stems and leaves samples further to clarify the release characteristic of flavonoids in SSF. The typical infrared characteristic

absorption peaks of samples were determined at 3139, 1559, 1403, 1311, 1075 and 543 cm^{-1} (Fig. 9c). Specifically, the strong and extensive absorption spectra observed at 3139 cm^{-1} were linked to the bending and stretching vibrations of the O–H group, a common finding in cellulose and hemicellulose constituents [41]. About FGSL, the absorption peak intensities at 1559 cm^{-1} and 1403 cm^{-1} were markedly diminished (due to the bending vibration of N–H from the lignin benzene ring and symmetrical CH_2 bending groups in cellulose), suggesting that the hydrogen bond of FGSL could be broken by the carbohydrate hydrolases [42, 43]. The angular vibration of cellulose's CH_3 symmetrical bond produced the absorption peak at around 1311 cm^{-1} [44]. The band at approximately 1075 cm^{-1} for the unfermented and fermented samples represented the stretching of the C–O–C vibration bond. At around 543 cm^{-1} , the β -glycosidic linkages between the glucose, cellulose, and hemicellulose sugar polymers were formed [44]. The peak strength dropped following SSF, suggesting that cellulose or hemicellulose's intermolecular hydrogen bonds had been disrupted.

Conclusion

This study established a rapid and non-destructive detection method for flavonoids in fermented *Glycyrrhiza* stems and leaves based on near-infrared spectroscopy and investigated the effects of fermentation on the flavonoid content, antioxidant capacity, metabolomics, structure, and enzyme activity of *Glycyrrhiza* stems and leaves. Based on the PLSR model, the optimal spectral preprocessing method was screened, and the R_p^2 and RMSEP of the optimal flavonoid model obtained were 0.9874 and 0.125, respectively. The external verification results indicate that the prediction model is highly accurate. Solid state fermentation significantly increased the content of flavonoids and the scavenging ability of DPPH free radical and hydroxyl free radical, reducing power. Additionally, a total of 461 secondary metabolites and 3 key differential metabolic pathways were successfully identified by UPLC-MS/MS metabolomics, mainly flavonoids and phenolic acids. Combined with FGSL and GSL thermogravimetric analysis and FTIR spectral results, the release of flavonoids may be associated with cellulose degradation caused by CMCase, xylanase, and α -amylase secretion, which contributes to the practical antioxidant effects of FGSL. Overall, the present study is essential in using fermented *Glycyrrhiza* stems and leaves flavonoids. Moreover, the findings of this study also provide new insights into understanding the release and biotransformation mechanism of flavonoids from *Glycyrrhiza* stems and leaves by SSF.

Supplementary Information

The online version contains supplementary material available at <https://doi.org/10.1186/s40538-024-00631-8>.

Supplementary Material 1.

Acknowledgements

This work was supported financially by Inner Mongolia Autonomous Region Doctoral Research Innovation Project (B20231064Z); Program of National Center of Technology Innovation for Dairy (2022- scientific research-2, 2023-QNRC-10); Major Science and Technology Program of Inner Mongolia Autonomous Region (2021ZD0023-3, 2021ZD0024-4).

Author contributions

Juan Du: writing—review and editing, writing—original draft, supervision, resources, project administration, methodology, investigation, formal analysis, data curation, conceptualization. Xia Li: methodology, formal analysis, data curation. Na Liu: investigation, formal analysis, conceptualization. Yuan Wang: methodology, formal analysis, data curation. Yaqian Li: methodology, formal analysis, data curation. Yang Jia: validation, software, formal analysis. Xiaoping An: writing—review and editing, supervision, project administration, investigation, funding acquisition, data curation, conceptualization. Jingwei Qi: writing—review and editing, supervision, resources, project administration, investigation, funding acquisition, data curation, conceptualization. All authors reviewed the manuscript.

Availability of data and materials

No datasets were generated or analyzed during the current study.

Declarations

Competing interests

The authors declare that there are no competing interests.

Author details

¹College of Animal Science, Inner Mongolia Agricultural University, Hohhot 010018, China. ²Key Laboratory of Smart Animal Husbandry at Universities of Inner Mongolia Autonomous Region/Integrated Research Platform of Smart Animal Husbandry at Universities of Inner Mongolia Autonomous Region/Inner Mongolia Herbivorous Livestock Feed Engineering Technology Research Center/National Center of Technology Innovation for Dairy-Breeding and Production Research Center, Hohhot 010018, China. ³Inner Mongolia Shengmu Animal Husbandry Co., Ltd., Hohhot 010020, China. ⁴Baotou Beichen Feed and Technology Inc., Baotou 014040, China.

Received: 8 April 2024 Accepted: 24 July 2024

Published online: 02 August 2024

References

- Sharifi-Rad J, Quispe C, Herrera-Bravo J, Belén LH, Kaur R, Kregiel D, et al. *Glycyrrhiza* genus: enlightening phytochemical components for pharmacological and health-promoting abilities. *Oxid Med Cell Longev*. 2021;2021:1–20. <https://doi.org/10.1155/2021/7571132>.
- Shang Z, Tian Y, Yi Y, Li K, Qiao X, Ye M. Comparative bioactivity evaluation and chemical profiling of different parts of the medicinal plant *Glycyrrhiza uralensis*. *J Pharmaceut Biomed*. 2022;215: 114793. <https://doi.org/10.1016/j.jpba.2022.114793>.
- Jiang L, Akram W, Luo B, Hu S, Faruque MQ, Ahmad S, et al. Metabolomic and pharmacologic insights of aerial and underground parts of *Glycyrrhiza uralensis* Fisch. ex DC. for maximum utilization of medicinal resources. *Front Pharmacol*. 2021;2021:1306. <https://doi.org/10.3389/fphar.2021.658670>.
- Panche AN, Diwan AD, Chandra SR. Flavonoids: an overview. *J Nutr Sci*. 2016;5: e47. <https://doi.org/10.1017/jns.2016.41>.
- Núñez-Gómez V, González-Barrio R, Periago MJ. Interaction between dietary fibre and bioactive compounds in plant by-products: impact on bioaccessibility and bioavailability. *Antioxidants*. 2023;12(4):976. <https://doi.org/10.3390/antiox12040976>.
- Tlais AZ, Fiorino GM, Polo A, Filannino P, Di Cagno R. High-value compounds in fruit, vegetable and cereal byproducts: an overview of potential sustainable reuse and exploitation. *Molecules*. 2020;25(13):2987. <https://doi.org/10.3390/molecules25132987>.
- Bhanja Dey T, Chakraborty S, Jain KK, Sharma A, Kuhad RC. Antioxidant phenolics and their microbial production by submerged and solid-state fermentation process: a review. *Trends Food Sci Tech*. 2016;2016(53):60–74. <https://doi.org/10.1016/j.tifs.2016.04.007>.
- Guo N, Zhu YW, Jiang YW, Li HK, Liu ZM, Wang W, et al. Improvement of flavonoid aglycone and biological activity of mulberry leaves by solid-state fermentation. *Ind Crop Prod*. 2020;2020(148): 112287. <https://doi.org/10.1016/j.indcrop.2020.112287>.
- Zhao Q, Yan X, Yue Y, Yue T, Yuan Y. Improved flavonoid content in mulberry leaves by solid-state fermentation: metabolic profile, activity, and mechanism. *Innov Food Sci Emerg*. 2023;84: 103308. <https://doi.org/10.1016/j.ifset.2023.103308>.
- Eweys AS, Zhao YS, Darwesh OM. Improving the antioxidant and anticancer potential of *Cinnamomum cassia* via fermentation with *Lactobacillus plantarum*. *Biotechnol Rep*. 2022;36: e00768. <https://doi.org/10.1016/j.btre.2022.e00768>.
- Wang Y, Li T, Li L, Ning J, Zhang Z. Micro-NIR spectrometer for quality assessment of tea: comparison of local and global models. *Spectrochim Acta A*. 2020;237: 118403. <https://doi.org/10.1016/j.saa.2020.118403>.
- Zaukuu JLZ, Benes E, Bázár G, Kovács Z, Fodor M. Agricultural potentials of molecular spectroscopy and advances for food authentication: an overview. *Processes*. 2022;10(2):214. <https://doi.org/10.3390/pr10020214>.
- Du J, Song Y, Li X, Liu N, An X, Qi J. Dynamic changes and correlation analysis of polysaccharide content and color parameters in *Glycyrrhiza* stems and leaves during fermentation. *Fermentation-Basel*. 2023;9(10):900. <https://doi.org/10.3390/fermentation9100900>.
- Yuan X, He C, Xue X, Liang Z, Chen Y. Optimisation study on the flavonoid extraction process from *Abrus precatorius* leaves and the comparison of total flavonoid content by HPLC and UV. *J Holist Integr Pharm*. 2023;4(2):119–26. <https://doi.org/10.1016/j.jhip.2023.09.003>.
- Sun Z, Su R, Qiao J, Zhao Z, Wang X. Flavonoids extraction from *Taraxacum officinale* (Dandelion): optimisation using response surface methodology and antioxidant activity. *J Chem-Ny*. 2014;2014:1–7. <https://doi.org/10.1155/2014/956278>.
- Liu L, Zareef M, Wang Z, Li H, Chen Q, Ouyang Q. Monitoring chlorophyll changes during Tencha processing using portable near-infrared spectroscopy. *Food Chem*. 2023;2023(412): 135505. <https://doi.org/10.1016/j.foodchem.2023.135505>.
- Wang L, Sun X, Li F, Yu D, Liu X, Huang W, Zhan J. Dynamic changes in phenolic compounds, colour and antioxidant activity of mulberry wine during alcoholic fermentation. *J Funct Foods*. 2015;18:254–65. <https://doi.org/10.1016/j.jff.2015.07.013>.
- Zhong Z, Xing R, Liu S, Wang L, Cai S, Li P. The antioxidant activity of 2-(4 (or 2)-hydroxyl-5-chloride-1, 3-benzene-di-sulfanamide)-chitosan. *Eur J Med Chem*. 2008;43(10):2171–7. <https://doi.org/10.1016/j.ejmech.2007.10.018>.
- Jeddou KB, Chaari F, Maktouf S, Nouri-Ellouz O, Helbert CB, Ghorbel RE. Structural, functional, and antioxidant properties of water-soluble polysaccharides from potatoes peels. *Food Chem*. 2016;205:97–105. <https://doi.org/10.1016/j.foodchem.2016.02.108>.
- Liu N, Song M, Wang N, Wang Y, Wang R, An X, Qi J. The effects of solid-state fermentation on the content, composition and in vitro antioxidant activity of flavonoids from dandelion. *PLoS ONE*. 2020;15(9): e0239076. <https://doi.org/10.1371/journal.pone.0239076>.
- Chen G, Liu Y, Zeng J, Tian X, Bei Q, Wu Z. Enhancing three phenolic fractions of oats (*Avena sativa* L.) and their antioxidant activities by solid-state fermentation with *Monascus anka* and *Bacillus subtilis*. *J Cereal Sci*. 2020;2020(93): 102940. <https://doi.org/10.1016/j.jcs.2020.102940>.
- Wang T, Sheng K, Zhang Y, Jin S, Feng L, Wang L. Metabolomics analysis reveals the effect of fermentation on the chemical composition and antioxidant activity of *Paeonia lactiflora* root. *Heliyon*. 2024. <https://doi.org/10.1016/j.heliyon.2024.e28450>.

23. Wu J, He T, Wang Z, Mao J, Sha R. The dynamic analysis of non-targeted metabolomics and antioxidant activity of *Dendrobium officinale* Kimura et Migo by the synergistic fermentation of bacteria and enzymes. *LWT*. 2024;203: 116354. <https://doi.org/10.1016/j.lwt.2024.116354>.
24. Pan L, Zhu Q, Lu R, McGrath JM. Determination of sucrose content in sugar beet by portable visible and near-infrared spectroscopy. *Food Chem*. 2015;167:264–71. <https://doi.org/10.1016/j.foodchem.2014.06.117>.
25. Li L, Sheng X, Zan J, Yuan H, Zong X, Jiang Y. Monitoring the dynamic change of catechins in black tea drying by using near-infrared spectroscopy and chemometrics. *J Food Compos Anal*. 2023;119: 105266. [https://doi.org/10.1016/j.jfca.2023\(2023\).105266](https://doi.org/10.1016/j.jfca.2023(2023).105266).
26. Wang Y, Cui Q, Jin S, Zhuo C, Luo Y, Yu Y, et al. Tea Analyzer: a low-cost and portable tool for quality quantification of postharvest fresh tea leaves. *LWT-Food Sci Technol*. 2022;159: 113248. <https://doi.org/10.1016/j.lwt.2022.113248>.
27. Zhang J, Wang P, Tan C, Zhao Y, Zhu Y, Bai J, et al. Effects of *L. plantarum* dy-1 fermentation time on the characteristic structure and antioxidant activity of barley β -glucan in vitro. *Curr Res Food Sci*. 2022;5:125–30. <https://doi.org/10.1016/j.crfs.2021.12.005>.
28. Wang L, Luo Y, Wu Y, Wu Z. Impact of fermentation degree on phenolic compositions and bioactivities during the fermentation of guava leaves with *Monascus anka* and *Bacillus* sp. *J Funct Foods*. 2018;41:183–90. <https://doi.org/10.1016/j.jff.2017.12.044>.
29. Li Y, Zhang Y, Dong L, Li Y, Liu Y, Liu Y, et al. Fermentation of *Lactobacillus fermentum* NB02 with feruloyl esterase production increases the phenolic compounds content and antioxidant properties of oat bran. *Food Chem*. 2024;437: 137834. <https://doi.org/10.1016/j.foodchem.2023.137834>.
30. Xiao J, Gu C, He S, Zhu D, Huang Y, Zhou Q. Widely targeted metabolomics analysis reveals new biomarkers and mechanistic insights on the chestnut (*Castanea mollissima* Bl.) calcification process. *Food Res Int*. 2021;141: 110128. <https://doi.org/10.1016/j.foodres.2021.110128>.
31. Li J, Hossain MS, Ma H, Yang Q, Gong X, Yang P, et al. Comparative metabolomics reveals differences in flavonoid metabolites among different coloured buckwheat flowers. *J Food Compos Anal*. 2020;2020(85): 103335. <https://doi.org/10.1016/j.jfca.2019.103335>.
32. Acosta-Estrada BA, Gutierrez-Urbe JA, Serna-Saldívar SO. Bound phenolics in foods, a review. *Food Chem*. 2014;152:46–55. <https://doi.org/10.1016/j.foodchem.2013.11.093>.
33. Si J, Xie J, Zheng B, Xie J, Chen Y, Yang C, et al. Release characteristic of bound polyphenols from tea residues insoluble dietary fiber by mixed solid-state fermentation with cellulose degrading strains CZ-6 and CZ-7. *Food Res Int*. 2023;173: 113319. <https://doi.org/10.1016/j.foodres.2023.113319>.
34. McCue PP, Shetty K. A role for amylase and peroxidase-linked polymerization in phenolic antioxidant mobilization in dark-germinated soybean and implications for health. *Process Biochem*. 2004;39(11):1785–91. <https://doi.org/10.1016/j.procbio.2003.08.007>.
35. Wang L, Zhang J, Zhang W, Lin X, Li C, Wu Z. Role of carbohydrate-cleaving enzymes in the phenolic mobilization of guava leaves tea during solid-state bio-processing with *Monascus anka* and *Bacillus* sp. *Process Biochem*. 2019;82:51–8. <https://doi.org/10.1016/j.procbio.2019.04.003>.
36. Chen Y, Wang Y, Chen J, Tang H, Wang C, Li Z, Xiao Y. Bioprocessing of soybeans (*Glycine max* L.) by solid-state fermentation with *Eurotium cristatum* YL-1 improves total phenolic content, isoflavone aglycones, and antioxidant activity. *Rsc Adv*. 2020;10(29):16928–41. <https://doi.org/10.1039/c9ra10344a>.
37. Xie J, Liu S, Dong R, Xie J, Chen Y, Peng G, et al. Bound polyphenols from insoluble dietary Fiber of defatted Rice bran by solid-state fermentation with *Trichoderma viride*: Profile, activity, and release mechanism. *J Agric Food Chem*. 2021;69(17):5026–39. <https://doi.org/10.1021/acs.jafc.1c00752>.
38. Xiao Y, Wu X, Yao X, Chen Y, Ho CT, He C, et al. Metabolite profiling, antioxidant and α -glucosidase inhibitory activities of buckwheat processed by solid-state fermentation with *Eurotium cristatum* YL-1. *Food Res Int*. 2021;143: 110262. <https://doi.org/10.1016/j.foodres.2021.110262>.
39. Li Y, Niu L, Guo Q, Shi L, Deng X, Liu X, et al. Effects of fermentation with lactic bacteria on the structural characteristics and physicochemical and functional properties of soluble dietary fiber from prosomillet bran. *LWT-Food Sci Technol*. 2022;2022(154): 112609. <https://doi.org/10.1016/j.lwt.2021.112609>.
40. Navarro-González I, García-Valverde V, García-Alonso J, Periago MJ. Chemical profile, functional and antioxidant properties of tomato peel fibre. *Food Res Int*. 2011;44(5):1528–35. <https://doi.org/10.1016/j.foodres.2011.04.005>.
41. Jia M, Chen J, Liu X, Xie M, Nie S, Chen Y, et al. Structural characteristics and functional properties of soluble dietary fibre from defatted rice bran obtained through *Trichoderma viride* fermentation. *Food Hydrocolloids*. 2019;2019(94):468–74. <https://doi.org/10.1016/j.foodhyd.2019.03.047>.
42. Loow YL, Wu TY, Lim YS, Tan KA, Siow LF, Jahim JM, et al. Improvement of xylose recovery from the stalks of oil palm fronds using inorganic salt and oxidative agent. *Energy Convers Manage*. 2017;138:248–60. <https://doi.org/10.1016/j.enconman.2016.12.015>.
43. Huang H, Chen J, Hu X, Chen Y, Xie J, Ao T, et al. Elucidation of the interaction effect between dietary fibre and bound polyphenol components on the anti-hyperglycemic activity of tea residue dietary fibre. *Food Funct*. 2022;13(5):2710–28. <https://doi.org/10.1039/D1FO03682C>.
44. Akpabli-Tsigbe NDK, Ma Y, Ekumah J-N, Osabutey J, Hu J, Xu M, et al. Novel solid-state fermentation extraction of 5-O-caf-feoylquinic acid from heilong48 soybean using *Lactobacillus Leviticus*: Parametric Screening and optimization. *LWT-Food Sci Technol*. 2021;2021(149): 111809. <https://doi.org/10.1016/j.lwt.2021.111809>.

Publisher's Note

Springer Nature remains neutral with regard to jurisdictional claims in published maps and institutional affiliations.